Preprints of the 21st IFAC World Congress (Virtual)
Berlin, Germany, July 12-17, 2020

Secondary Control of Microgrids via Neural Inverse Optimal Distributed Cooperative Control ⋆

Carlos J. Vega * **Larbi Djilali** * **Edgar N. Sanchez** *

* *Electrical Engineering Department, CINVESTAV, Guadalajara. Av. del Bosque 1145, Col. El Bajio, Zapopan, 45019, México, (e-mail: {cjvega, ldjilali, sanchez}@gdl.cinvestav.mx).*

Abstract: In this paper, a new control scheme of secondary voltage and frequency control based on a discrete-time neural inverse optimal distributed cooperative structure is proposed for islanded microgrids. A neural adaptive secondary controller for each distributed generator is developed to achieve the desired goals. The proposed controllers are composed of an on-line neural identification scheme on the basis of a recurrent high-order neural network using the extended Kalman filter and a nonlinear control strategy. Additionally, the proposed control scheme does not require information of all installed distributed generators neither a distributed generator model, which improves reliability. The proposed controllers are validated through simulation for an islanded AC microgrid.

Keywords: Distributed energy sources, Distributed cooperative control, Inverse optimal control, Islanded AC microgrid, Neural networks.

1. INTRODUCTION

Nowadays, microgrids provide an efficient solution to ensure better use of Distributed Energy Resource (DER), to improve operation and stability of the electrical grid. A microgrid is composed of different Distributed Generators (DGs) such as wind power systems, solar power systems, small gas turbines, among others electrical generators,storage devices, and loads (Bidram et al. (2017.)). To ensure flexible power-sharing and high-injected power quality, the DERs are linked to the microgrid using power electronic converters (Yazdanian and Mehrizi-Sani (2014)). The hierarchical control scheme is extensively utilized for microgrids to ensure its adequate operation in two modes: grid-connected mode and islanded mode. (Guo et al. (2017.)), this scheme distributes the microgrid control objectives among three control levels as primary, secondary, and tertiary ones to achieve the required performances (Awal et al. (2020)).

In the hierarchical structure, the primary controller is used to achieve the tracking of voltages, currents, and powers, in which their desired values are obtained from the secondary layer (Pogaku et al. (2007)). This controller is installed at each DG in order to ensure power balance between power generation and the load (Awal et al. (2020)). The primary controller objectives are adequately achieved by using conventional controllers as the droop method, which can be implemented without communication links between the microgrid subsystems (Sadeghkhani et al. (2018), Djilali et al. (2019)). This technique has been used widely for microgrid applications in islanded mode Han et al. (2016), Sun et al. (2017). In Han et al. (2015), an improved droop control method is proposed where two operations are included which are error reduction operation and voltage recovery one. In Guerrero et al. (2004) an enhanced droop control is investigated to improve transient droop performances. To improve the generated active and reactive power decoupling, enhanced droop controllers are developed in Chiang et al. (2001).

For island microgrid, the microgrid voltage amplitude and frequency should be maintained at predefined values in the presence of different operation conditions as explained in Shen et al. (2019). The secondary controller should set the generated active and reactive power for each DG regarding the voltage amplitude and frequency deviations. In Sadeghkhani et al. (2018), a voltage and current controllers and a modified droop method are used to design primary and secondary level control; the latter one is used to regulate the reactive power desired value. In Lee et al. (2018), primary and secondary layers are developed such that the primary control based on the droop controller deals with power regulations, while the secondary one consists of a dynamics consensus algorithm, which is utilized to ensure the microgrid permanent connection to the main grid. Awal et al. (2020), a hierarchical control structure for virtual oscillator control based microgrids is investigated for both islanded and grid-connected modes such that in islanded mode, a voltage and frequency regulation and grid synchronization is proposed, while in grid-connected mode, a method for power reference tracking is developed.

To ensure adequate sharing of the generated active and reactive power, using local controllers, and restore and maintain voltage amplitude and frequency of the islanded microgrid at the rated values, using the secondary controllers, are very difficult due to the complexes dynamics

⋆ This work is supported by CONACYT, Mexico, Project 257200.

and inspected behaviors of loads as demonstrated in Han et al. (2016). To solve the reactive power sharing problem, different works have been developed as in Mahmood et al. (2015) where an adaptive voltage droop control is presented. This method provides a good solution for reactive power-sharing; however, nonlinear and unbalanced loads are not considered. Another method is developed in He and Li (2012), where active power disturbances are used to identify the error of the reactive power sharing and eliminate it by using a slow integral term; however, this method affects power quality and can lead to instability. In Li et al. (2015), an adaptive inverse improved droop control is proposed to regulate unbalanced power and reactive power sharing; unfortunately, for islanded microgrid sharing reactive power is hard to ensure in presence of nonlinear and unbalanced load conditions.

Recently, neural networks present a potential method for implementing nonlinear system identification and control due to their capabilities to approximate complex dynamics, which help to improve control scheme performances (Sanchez et al. (2008)). In this paper, an islanded AC microgrid controlled on the basis of neural distributed cooperative controller is presented. The main contribution of the present paper are summarized: 1) a distributed cooperative secondary controller-based discrete-time Neural inverse Optimal Control (N-IOC) is proposed for each DG. 2) To identify the unknown discrete-time nonlinear models, Recurrent High Order Neural Networks (RHONN) are utilized, which are a kind of special neural networks with many useful dynamical properties (Kosmatopoulos et al. (1997)). 3) The RHONN identifier is trained on-line with an Extended Kalman Filter (EKF) Sanchez et al. (2008), i.e., the controller is a free-model technique. 4) Since, the proposed secondary control is based on the pinning technique, all DGs are synchronized to a desired reference by means of a simple communication network, which leads to system reliability enhancement.

This paper is organized as follows. The microgrid control structure is presented in Section 2. Section 3 proposes the main paper contribution, related to development and design of the proposed control scheme. The selected microgrid test system and the obtained results are discussed in Section 4. Finally, conclusions are stated in Section 5.

2. MICROGRID CONTROL STRUCTURE

Figure 1 displays the proposed hierarchical control structure for an AC microgrid to ensure adequate operation in islanded mode. The proposed control scheme is composed of an inner loop controller (primary control) and an outer loop one (secondary control); both controllers are applied for the voltage source inverters (VSI) of DGs.

The primary controller regulates voltage and frequency of the microgrid for the operating modes (grid-connected mode and islanded mode). The goal of this layer is to prevent voltage and frequency failures. Nevertheless, this controller is insufficient to ensure normal operating conditions of the microgrid, requiring an additional control level to compensate voltage and frequency deviation. The secondary control level responds in a slower timescale, which allows decoupling between the primary and the secondary control layers and simplifies their designs. Generally, the

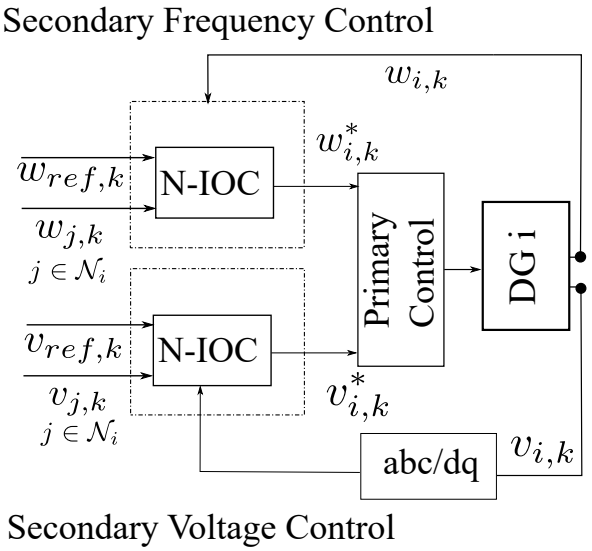

Fig. 1. Block diagram of the proposed distributed cooperative hierarchical control of a microgrid.

control strategies of the secondary controllers are VF control, PQ control, and droop control (Kim et al. (2010)). In this paper, the proposed scheme for the secondary control level is Voltage-Frequency neural inverse optimal distributed cooperative control. The proposed secondary controller for each DG requires minimal information from neighbors. This control adapts to changes in the DG parameters, loads, and microgrid operating conditions. The proposed controller reacts to changes in the system, adjusting the control parameters in real-time, due to the on-line neural identifier.

The primary control is usually implemented as a local controller at each DG. Development of the primary local controller is conventionally based on active and reactive power droop techniques. Droop technique relates the frequency and active power, and voltage amplitude and reactive power. Frequency and voltage droop characteristics for the i^{th} DG are given by

$$w_{i,k} = w^*_{i,k} - D_P P_{i,k}, \tag{1}$$

$$v_{o,mag,k} = v^*_{i,k} - D_Q Q_{i,k}. \tag{2}$$

The droop technique gives voltage references for the voltage control loop, implemented as a discrete-time proportional-integral (PI) controller, which adjusts current references for the current control loop. This latter loop manipulates the Sinusoidal Pulse Width Modulation (SPWM) algorithm of the inverter bridge, which is connected to a primary DC power source. The current control loop is designed as a discrete-time PI controller with feedforward signal and harmonics rejection filter.

3. PROPOSED DISTRIBUTED COOPERATIVE SECONDARY CONTROL

The objective of this controller is to determine the references trajectory for the primary control ($w^*_{i,k}$, $v^*_{i,k}$) to regulate frequency and voltage amplitude to their nominal values. For this goal, a neural adaptive and distributed secondary control for microgrids with inverter-based DG

is proposed. The DG nonlinear dynamical model and parameters are assumed to be unknown.

3.1 Secondary Frequency Control

The secondary frequency control of the i^{th} DG selects $w^*_{i,k}$ in (1) such that frequency amplitude $w_{i,k}$ of each DG , approaches the reference value, w_{ref}.

Assume that there is an unknown discrete-time dynamical model for $w_{i,k} = f(w^*_{i,k})$, which is formulated as a second-order nonlinear dynamical system, given by

$$\begin{aligned} x_{Wi,k+1} =& f_{Wi}(x_{Wi,k}) + g_{Wi}(x_{Wi,k})u_{Wi,k}, \\ y_{Wi,k} =& w_{i,k}, \quad \text{with} \quad u_{Wi,k} = w^*_{i,k}, \end{aligned}$$

where the state vector for each i^{th} DG inverter is $x_{Wi,k} = [w_{i,k}, \quad w_{i,k+1}]^T$, the vector functions $f_{Wi}(\cdot)$ and $g_{Wi}(\cdot)$ are unknown, with $x_{Wi,k}$ available for measurement.

The DGs are considered as nodes which exchange information among neighbors through a communication network. This communication network is modeled by a graph. The local neighborhood tracking error for each DG is defined by

$$e_{Wi,k} = \sum_{j\in\mathcal{N}_i} a_{ij}(y_{Wi,k} - y_{Wj,k}) + b_i(y_{Wi,k} - y_{W_0,k}), \quad (3)$$

where $\mathcal{N}_i$ denotes the set of DGs neighboring the i^{th} DG, a_{ij} denotes the elements of the communication adjacency matrix, and $y_{W_0,k} = [w_{ref,k}, \quad w_{ref,k+1}]^T$. b_i is the pinning gain by which the i^{th} DG is connected to the leader node, which is the reference one.

The dynamical equation of (3) is

$$\begin{aligned} e_{Wi,k+1} =& \sum_{j\in\mathcal{N}_i} a_{ij}(y_{Wi,k+1} - y_{Wj,k+1}) \\ &+ b_i(y_{Wi,k+1} - y_{W_0,k+1}) \quad (4) \\ =& d_i(f_{Wi}(x_{Wi,k}) + g_{Wi}(x_{Wi,k})u_{Wi,k}) - b_i y_{W_0,k+1} \\ &+ \sum_{j\in\mathcal{N}_i} a_{ij}(f_{Wj}(x_{Wj,k}) + g_{Wj}(x_{Wj,k})u_{Wj,k}) \end{aligned}$$

$$\text{with } d_i = b_i + \sum_{j\in\mathcal{N}_i} a_{ij}$$

$$\begin{aligned} e_{Wi,k+1} =& \tilde{F}_{Wi}(x_{Wi,k}) + \tilde{G}_{Wi}(x_{Wi,k})u_{Wi,k} \\ &+ \sum_{j\in\mathcal{N}_i} a_{ij}H_j(y_{Wj,k}) \end{aligned}$$

where the functions $\tilde{F}_{Wi}(\cdot)$ $\tilde{G}_{Wi}(\cdot)$, and $H_j(\cdot)$ are unknown. System (4) is identified by a neural identifier in a series-parallel structure, which is proposed as

$$\chi_{Wi,k+1} = \hat{F}_{Wi}(e_{Wi,k}) + \hat{G}_{Wi}u_{Wi,k} \quad (5)$$

where χ_{Wi} is the vector estimated by the neural identifier, $\hat{G}_{Wi} = [0, \quad \varpi_{Wi,2}]^T$, and

$$\hat{F}_{Wi}(e_{Wi,k}) = \left[\hat{f}_{Wi,1}(e_{Wi,k}), \quad \hat{f}_{Wi,2}(e_{Wi,k})\right]^T$$

is defined as

$$\begin{aligned} \hat{f}_{Wi,1}(e_{Wi,k}) =& \omega_{1,k}S(e_{Wi,1,k}) + e_{Wi,2,k} \\ =& \omega_{11,k}S(e_{Wi,1,k}) + \omega_{12,k}S^2(e_{wi,1,k}) + e_{Wi,2,k} \\ \hat{f}_{Wi,2}(e_{Wi,k}) =& \omega_{21,k}S(e_{Wi,2,k}) + \omega_{22,k}S(e_{Wi,1,k})S(e_{Wi,2,k}) \\ &+ \omega_{23,k}S^2(e_{Wi,2,k}) + \omega_{24,k}S^3(e_{Wi,2,k}) \end{aligned}$$

with $i = 1, \ldots, n$ is the DG numbers. For on-line RHONN weights adaptation, the EKF training algorithm is used (Sanchez et al. (2008)).

System (5) is an affine-in-the-input discrete-time nonlinear system. Furthermore, the discrete-time inverse optimal controller is designed Ornelas-Tellez et al. (2012) to stabilize (4), as

$$\begin{aligned} z_{Wi,1,k} =& e_{Wi,1,k} \\ V_{Wi,2,k} =& -\omega_{1,k}S(e_{Wi,1,k}) - K_{Wi,1}z_{Wi,1,k} \\ u^*_{Wi,k} =& -\frac{1}{2}\left(R + \frac{g_k^T P g_k}{2}\right)^{-1} g_k^T P(f_k - x_{d,k+1}) \\ =& -\frac{1}{3}(\hat{f}_{Wi,2}(e_{Wi,k}) - V_{Wi,2,k+1}) \end{aligned}$$

where $z_{Wi,1,k}$ is a auxiliary variable, $V_{Wi,2,k}$ is a virtual control, $0 < K_{Wi,1} < 1$ is a parameter design, and $u^*_{Wi,k}$ is a discrete-time inverse optimal control law, with $P = 1$, $R = 1$, $g_k = \varpi_{Wi,2} = 1$.

3.2 Secondary Voltage Control

The secondary voltage control of the i^{th} DG in the microgrid selects $v^*_{i,k}$ in (2) such that the voltage magnitude $v_{o,mag,k}$ of each DG , approaches the reference value, v_{ref}. The voltage magnitude for each i^{th} DG is

$$v_{o,mag,k} = \sqrt{v^2_{d,i,k} + v^2_{q,i,k}},$$

and the primary voltage control aligns the voltage magnitude on the d-axis of the corresponding reference frame ($v^2_{q,i,k} = 0$); furthermore, the secondary control goal is to design $v^*_{i,d,k}$ such that $v_{i,d,k} \to v_{ref}$, for all i.

For secondary frequency control, assume that there is an unknown discrete-time dynamical model $v_{i,d,k} = f(v^*_{i,d,k})$, which is formulated as a second-order nonlinear dynamical system, given by

$$\begin{aligned} x_{Vi,k+1} =& f_{Vi}(x_{Vi,k}) + g_{Vi}(x_{Vi,k})u_{Vi,k}, \\ y_{Vi,k} =& v_{i,d,k}, \quad \text{with} \quad u_{Vi,k} = v^*_{i,d,k}, \end{aligned}$$

where the state vector for each i^{th} DG inverter is $x_{Vi,k} = [v_{i,d,k}, \quad v_{i,d,k+1}]^T$, the vector functions $f_{Vi}(\cdot)$ and $g_{Vi}(\cdot)$ are unknown, with $x_{Vi,k}$ available for measurement.

For this case, the local neighborhood tracking error for each DG is defined by

$$e_{Vi,k} = \sum_{j\in\mathcal{N}_i} a_{ij}(y_{Vi,k} - y_{Vj,k}) + b_i(y_{Vi,k} - y_{V_0,k}), \quad (6)$$

where $y_{V_0,k} = [v_{ref,k}, \quad v_{ref,k+1}]^T$.

The dynamical equation of (6) is

$$\begin{aligned} e_{Vi,k+1} =& \sum_{j\in\mathcal{N}_i} a_{ij}(y_{Vi,k+1} - y_{Vj,k+1}) \\ &+ b_i(y_{Vi,k+1} - y_{V_0,k+1}) \quad (7) \\ =& \tilde{F}_{Vi}(x_{Vi,k}) + \tilde{G}_{Vi}(x_{Vi,k})u_{Vi,k} \\ &+ \sum_{j\in\mathcal{N}_i} a_{ij}H_j(y_{Wj,k}) \end{aligned}$$

where the functions $\tilde{F}_{Wi}(\cdot)$ $\tilde{G}_{Wi}(\cdot)$, and $H_j(\cdot)$ are unknown. System (7) is identified by a neural identifier in a series-parallel structure, which is proposed as

$$\chi_{Vi,k+1} = \hat{F}_{Vi}(e_{Vi,k}) + \hat{G}_{Vi}u_{Vi,k} \quad (8)$$

where χ_{Vi} is the vector estimated by the neural identifier, $\hat{G}_{Vi} = \hat{G}_{Wi}$, and

$$\hat{F}_{Vi}(e_{Vi,k}) = \hat{F}_{Wi}(e_{Wi,k})$$

The discrete-time inverse optimal controller is proposed Ornelas-Tellez et al. (2012) to stabilize (7), as

$$\begin{aligned} z_{Vi,1,k} =& e_{Vi,1,k} \\ V_{Vi,2,k} =& -\omega_{1,k} S(e_{Vi,1,k}) - K_{Vi,1} z_{Vi,1,k} \\ u^*_{Vi,k} =& -\frac{1}{3}(\hat{f}_{Vi,2}(e_{Vi,k}) - V_{Vi,2,k+1}) \end{aligned}$$

where $z_{Vi,1,k}$ is a auxiliary variable, $V_{Vi,2,k}$ is a virtual control, $0 < K_{Vi,1} < 1$ is a parameter design, and $u^*_{Vi,k}$ is a discrete-time inverse optimal control law, with $P = 1$, $R = 1$, $g_k = \varpi_{Wi,2} = 1$.

4. SIMULATION RESULTS

The proposed secondary voltage and frequency controllers, as well as the microgrid, are simulated using the SimPower System toolbox of Matlab [1]. The effectiveness of the proposed control scheme is verified by simulating a microgrid in island operation mode composed of four DGs, Figure 2. The parameter of the proposed microgrid are illustrated

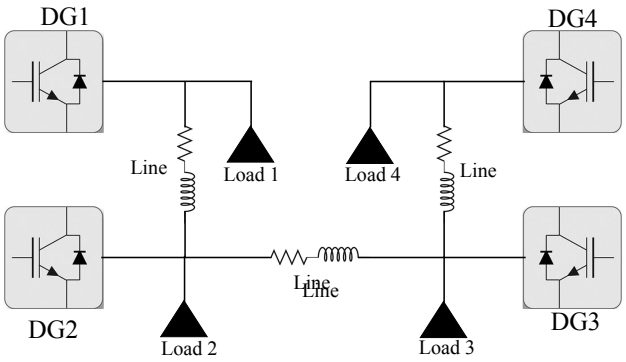

Fig. 2. Microgrid selected structure.

in Table. 1 The proposed secondary controller is used to

Table 1. The microgrid equipment sizing and parameters.

DERs	Equipment	Parameters
DG 1 to DG4	DG: S, V_{dc}, F	$100kVA$, $500V$, $60Hz$
	LC filter: R, L, C	0.03Ω, $0.35mH$, $50\mu F$
Line 1 to 3	R, L	0.23Ω, $0.318mH$
Loads 1 to 4	P_L, Q_L	$100kW$, $24kVAr$

deal with grid voltage and frequency deviations. In case of microgrid voltage amplitude and frequency disturbances, this controller sets the desired values of the active and reactive power, which should be injected by each DG into the microgrid. The selected powers values are tracked using the primary DG controller. Since the proposed control scheme is based on pinning control, all nodes (DGs) are synchronized to the leader one, which is in the present case the DG 1. This leader node shares the information by means of a communication network with the other DGs (DG2-DG4), hence, all the installed DGS references are synchronized.

[1] Matlab, Simulink. de 1994-2018, ©The Math Works, Inc.

Figure 3 displays the dynamics of the $d-q$ voltage in (pu) for each DG. The $-d-$ lines voltage (black) of each DG are forced to track constant amplitude $1pu$ (red), while the The $-q-$ lines voltage (blue) is maintained at zero. Figure 4 presents the frequency desired values (red)

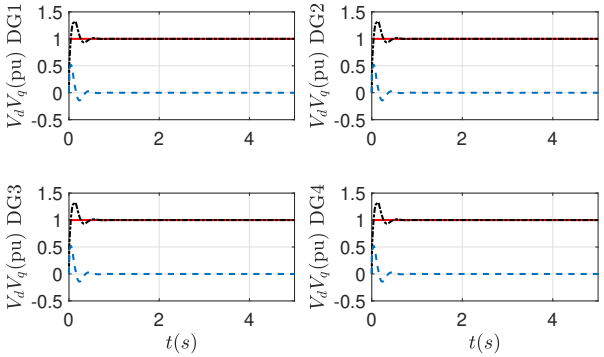

Fig. 3. The $d-q$ voltage and reference, DGi, $i = 1, \ldots, 4$: $v_{d,i,k}$ (black line), $v_{q,i,k}$ (blue line), v_{ref} (red line).

and the real one at each DG (black). The active (blue)

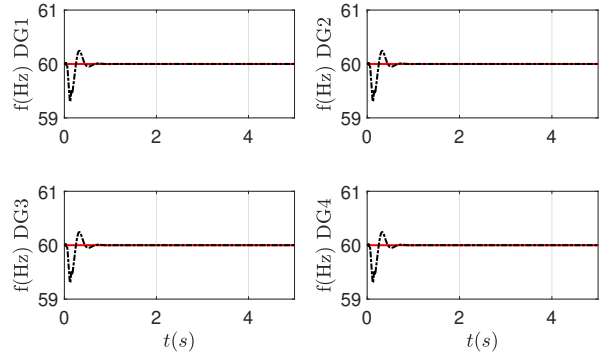

Fig. 4. Frequency DGi, $i = 1, \ldots, 4$: $w_{i,k}$ (black line), w_{ref} (red line).

and reactive (black) power desired values of each DG which are obtained from the proposed secondary control scheme are presented at Figure.5. These desired power trajectories are tracked using the primary controllers. Since the microgrid is simulated considering balanced loads conditions, the active power desired values is $1pu$ ensures a nominal frequency value of $60Hz$, and the reactive power desired value is zero assures a microgrid nominal voltage amplitude value. Figure 6 and Figure 7 illustrate the three-phase voltage and currents lines for each DG (pu), respectively. From the obtained results, it is clear that the proposed control scheme achieves the control objectives where the rated voltage amplitude and frequency are ensured. In addition, an adequate decoupling between the $d-q$ voltage axes, and active and reactive power is carried-out, which guarantee a flexible power-sharing.

5. CONCLUSIONS

In this paper, secondary voltage and frequency controllers, based on a discrete-time neural inverse optimal distributed

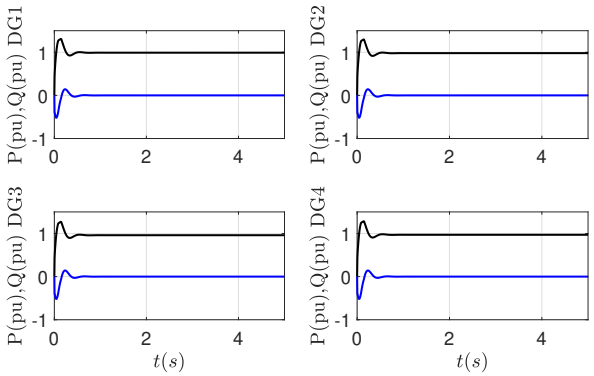

Fig. 5. Active and reactive power DGi, $i = 1, \ldots, 4$: $P_{i,k}$ (black line), $Q_{i,k}$ (blue line).

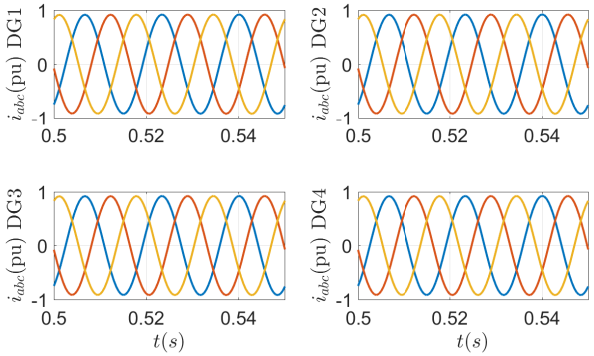

Fig. 6. Three-phase currents, DGi, $i = 1, \ldots, 4$.

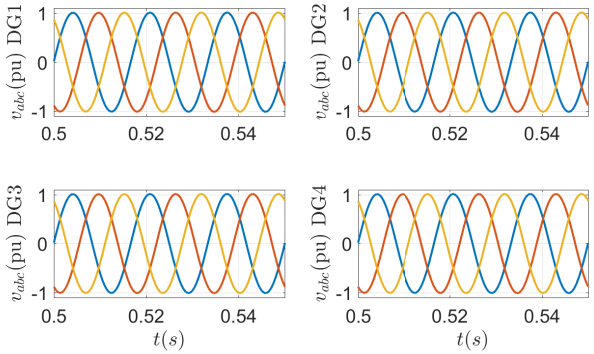

Fig. 7. Three-phase Voltages DGi, $i = 1, \ldots, 4$.

cooperative scheme are developed for islanded AC microgrids. The proposed controllers are used to generate the reference trajectories for the primary level control. Since they are based on RHONN identifiers, trained on-line with an EKF, which allows adjusting indirectly the control algorithm in real-time, DGs mathematical models are not required. Additionally, thanks to the pinning control technique, all nodes (DGs) are synchronized to a leader one, which is the reference, and is connected to a minimal number of DGs; it shares the information with its neighbors through of a simple communication network. The proposed scheme is developed for a microgrid in island operation mode and is verified via simulation. The obtained results illustrate the effectiveness of the proposed control scheme to ensure the required voltage amplitude and frequency in the microgrid. In addition, adequate active and reactive power sharing is achieved.

REFERENCES

Awal, M.A., Yu, H., Tu, H., Lukic, S.M., and Husain, I. (2020). Hierarchical control for virtual oscillator based grid-connected and islanded microgrids. *IEEE Transactions on Power Electronics*, 35(1), 988–1001.

Bidram, A., Nasirian, V., Davoudi, A., and Lewis, F.L. (2017.). *Cooperative Synchronization in Distributed Microgrid Control*. Springer, Cham, Switzerland.

Chiang, S., Yen, C., and Chang, K. (2001). A multimodule parallelable series-connected pwm voltage regulator. *IEEE Transactions on Industrial Electronics*, 48(3), 506–516.

Djilali, L., N.Sanchez, E., Ornelas-Tellez, F., Avalos, A., and Belkheiri, M. (2019). Improving microgrid low-voltage ride-through capacity using neural control. *IEEE Systems Journal (Early Access)*.

Guerrero, J., de Vicma, L., Castilla, M., and J.Miret (2004). A wireless controller to enhance dynamic performance of parallel inverters in distributed generation system. *IEEE Transactions on Power Electronics*, 19(5), 1205–1213.

Guo, F., Wen, C., and Song, Y.D. (2017.). *Distributed Control and Optimization Technologies in Smart Grid Systems*. CRC Press, Boca Raton, FL, USA.

Han, H., Liu, Y., Sun, Y., Su, M., and Guerrero, J.M. (2015). An improved droop control strategy for reactive power sharing in islanded microgrid. *IEEE Transactions on Power Electronics*, 30(6), 3133–3141.

Han, Y., Li, H., Shen, P., Coelho, E.A.A., and Guerrero, J.M. (2016). Review of active and reactive power sharing strategies in hierarchical controlled microgrids. *IEEE Transactions on Power Electronics*, 32(3), 2427–2451.

He, J.W. and Li, Y.W. (2012). An enhanced microgrid load demand sharing strategy. *IEEE Transactions on Power Electronics*, 27(9), 3984–3995.

Kim, J.Y., Jeon, J.H., Kim, S.K., Cho, C., Park, J.H., Kim, H.M., and Nam, K.Y. (2010). Cooperative control strategy of energy storage system and microsources for stabilizing the microgrid during islanded operation. *IEEE Transactions on Power Electronics*, 25(12), 3037–3048.

Kosmatopoulos, E.B., Christodoulou, M.A., and Ioannou, P.A. (1997). Dynamical neural networks that ensure exponential identification error convergence. *Neural Networks*, 10(2), 299–314.

Lee, W.G., Nguyen, T.T., Yoo, H.J., and Kim, H.M. (2018). Low-voltage ride-through operation of grid-connected microgrid using consensus-based distributed control. *Energies*, 11(11), :2867.

Li, P., Wang, B., Lee, W.J., and Xu, D. (2015). Dynamic power conditioning method of microgrid via adaptive inverse control. *IEEE Transactions on Powers Delivery*, 30(2), 906–913.

Mahmood, H., Michaelson, D., and Jiang, J. (2015). Reactive power sharing in island microgrids using adaptive voltage droop control. *IEEE Transactions on Smart Grid*, 6(6), 3052–3060.

Ornelas-Tellez, F., Sanchez, E.N., and Loukianov, A.G. (2012). Discrete-time neural inverse optimal control for nonlinear systems via passivation. *IEEE Transactions*

on Neural Networks and Learning Systems, 23(8), 1327–1339.

Pogaku, N., Prodanovic, M., and Green, T.C. (2007). Modeling, analysis and testing of autonomous operation of an inverter-based microgrid. *IEEE transactions on Power electronics*, 22(2), 613–625.

Sadeghkhani, I., Golshan, M.E., Mehrizi-Sani, A., and Guerrero, J.M. (2018). Low-voltage ride-through of a droop-based three-phase four-wire grid-connected microgird. *IET Generation, Transmission & Distribution*, 12(8), 1906–1914.

Sanchez, E.N., Alanís, A.Y., and Loukianov, A.G. (2008). *Discrete-time high order neural control: trained with Kalman filtering*, volume 112. Springer Science & Business Media.

Shen, X., Wang, H., Li, J., Su, Q., and Gao, L. (2019). Distributed secondary voltage control of islanded microgrids based on rbf-neural- network sliding-mode technique. *IEEE Access*, 7, 65616–65623.

Sun, Y., Hou, X., Yang, J., Han, H., Su, M., and Guerrero, J.M. (2017). New perspectives on droop control in ac microgrid. *IEEE Transactions on Industrial Electronics*, 64(7), 5741–5745.

Yazdanian, M. and Mehrizi-Sani, A. (2014). Distributed control techniques in microgrids. *IEEE Trans. Smart Grid*, 5(6), 2901–2909.